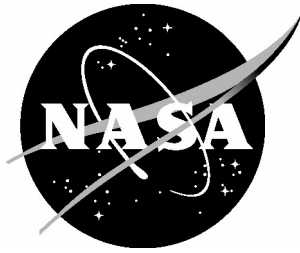


NASA/CR-2004-213241



An Inviscid Computational Study of the Space Shuttle Orbiter and Several Damaged Configurations

Ramadas K. Prabhu

Lockheed Martin Engineering & Sciences Company, Hampton, Virginia

The NASA STI Program Office . . . in Profile

Since its founding, NASA has been dedicated to the advancement of aeronautics and space science. The NASA Scientific and Technical Information (STI) Program Office plays a key part in helping NASA maintain this important role.

The NASA STI Program Office is operated by Langley Research Center, the lead center for NASA's scientific and technical information. The NASA STI Program Office provides access to the NASA STI Database, the largest collection of aeronautical and space science STI in the world. The Program Office is also NASA's institutional mechanism for disseminating the results of its research and development activities. These results are published by NASA in the NASA STI Report Series, which includes the following report types:

- **TECHNICAL PUBLICATION.** Reports of completed research or a major significant phase of research that present the results of NASA programs and include extensive data or theoretical analysis. Includes compilations of significant scientific and technical data and information deemed to be of continuing reference value. NASA counterpart of peer-reviewed formal professional papers, but having less stringent limitations on manuscript length and extent of graphic presentations.
- **TECHNICAL MEMORANDUM.** Scientific and technical findings that are preliminary or of specialized interest, e.g., quick release reports, working papers, and bibliographies that contain minimal annotation. Does not contain extensive analysis.
- **CONTRACTOR REPORT.** Scientific and technical findings by NASA-sponsored contractors and grantees.

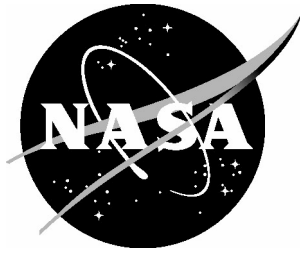
- **CONFERENCE PUBLICATION.** Collected papers from scientific and technical conferences, symposia, seminars, or other meetings sponsored or co-sponsored by NASA.
- **SPECIAL PUBLICATION.** Scientific, technical, or historical information from NASA programs, projects, and missions, often concerned with subjects having substantial public interest.
- **TECHNICAL TRANSLATION.** English-language translations of foreign scientific and technical material pertinent to NASA's mission.

Specialized services that complement the STI Program Office's diverse offerings include creating custom thesauri, building customized databases, organizing and publishing research results ... even providing videos.

For more information about the NASA STI Program Office, see the following:

- Access the NASA STI Program Home Page at [*http://www.sti.nasa.gov*](http://www.sti.nasa.gov)
- E-mail your question via the Internet to [*help@sti.nasa.gov*](mailto:help@sti.nasa.gov)
- Fax your question to the NASA STI Help Desk at (301) 621-0134
- Phone the NASA STI Help Desk at (301) 621-0390
- Write to:
NASA STI Help Desk
NASA Center for AeroSpace Information
7121 Standard Drive
Hanover, MD 21076-1320

NASA/CR-2004-213241



An Inviscid Computational Study of the Space Shuttle Orbiter and Several Damaged Configurations

Ramadas K. Prabhu

Lockheed Martin Engineering & Sciences Company, Hampton, Virginia

National Aeronautics and
Space Administration

Langley Research Center
Hampton, Virginia 23681-2199

Prepared for Langley Research Center
under Contract NAS1-00135

July 2004

Available from:

NASA Center for AeroSpace Information (CASI)
7121 Standard Drive
Hanover, MD 21076-1320
(301) 621-0390

National Technical Information Service (NTIS)
5285 Port Royal Road
Springfield, VA 22161-2171
(703) 605-6000

Summary

Inviscid aerodynamic characteristics of the Space Shuttle Orbiter were computed in support of the Columbia Accident Investigation. The unstructured grid software FELISA was used and computations were done using freestream conditions corresponding to those in the NASA Langley 20-Inch Mach 6 CF_4 tunnel test section. The angle of attack was held constant at 40 degrees. The baseline (undamaged) configuration and a large number of damaged configurations of the Orbiter were studied. Most of the computations were done on a half-model. However, one set of computations was done using the full-model to study the effect of sideslip. The differences in the aerodynamic coefficients for the damaged and the baseline configurations were computed. Simultaneously with the computation reported here, tests were being done on a scale model of the Orbiter in the 20-Inch Mach 6 CF_4 tunnel to measure the ‘deltas’. The present computations complemented the CF_4 tunnel test, and provided aerodynamic coefficients of the Orbiter as well as its components. Further, they also provided details of the flow field.

Nomenclature

C_X	$\mathbf{F}_X / (q_\infty S_{ref})$
C_Y	$\mathbf{F}_Y / (q_\infty S_{ref})$
C_Z	$\mathbf{F}_Z / (q_\infty S_{ref})$
CM_X	$\mathbf{M}_X / (q_\infty S_{ref} b_{ref})$
CM_Y	$\mathbf{M}_Y / (q_\infty S_{ref} c_{ref})$
CM_Z	$\mathbf{M}_Z / (q_\infty S_{ref} b_{ref})$
\mathbf{F}_X	Force along the x-axis
\mathbf{F}_Y	Force along the y-axis
\mathbf{F}_Z	Force along the z-axis
\mathbf{M}_X	Moment about the x-axis
\mathbf{M}_Y	Moment about the y-axis
\mathbf{M}_Z	Moment about the z-axis
b_{ref}	Reference length for CM_X and CM_Z
c_{ref}	Reference length for CM_Y
M_∞	Freestream Mach number
q_∞	Freestream dynamic pressure
S_{ref}	Reference area
T_∞	Freestream temperature
V_∞	Freestream velocity
x, y, z	Cartesian co-ordinates of a given point
α	Angle of attack, degrees
β	Sideslip angle, degrees
γ	Isentropic index
$\delta()$	Difference in aero coefficients for the damaged and the baseline
ρ_∞	Freestream density

Introduction

This report documents the results of a computational study done in support of the Space Shuttle Columbia accident investigation. The Columbia Accident Investigation Board report¹ concluded that the cause of the accident was a breach in the TPS on the leading edge of the port wing. This breach was caused by the

impact of a piece of insulation foam that had separated from the external tank soon after lift-off. During reentry, this breach led to the weakening of the wing, and ultimately to the loss of the vehicle.

Examination of the Orbiter trajectory and the recorded flight data (during the re-entry until the loss of the signal) showed deviations in the aerodynamic coefficients as compared to the undamaged vehicle (for the known Mach number, angle of attack, sideslip, and control deflections). These deviations in aerodynamic coefficients, called the ‘deltas’, were very small at the time of Orbiter’s entry into atmosphere, but increased gradually reaching catastrophic values at the end. In addition, a couple of hot-spots had been noticed on the left side of the fuselage, possibly due to the hot gases that may have escaped from under the wing to the upper side. In order to investigate these observations, tests were done on a scale model at the NASA Langley Research Center in the 20-inch Mach 6 CF_4 Tunnel which simulates flight conditions at high Mach numbers. These tests were done on the baseline and several damaged configurations, and the ‘deltas’ for the damaged configurations were evaluated from the data.

The purpose of the present study was to complement the CF_4 tunnel tests, and compute the ‘deltas’ to assist in the reconstruction of a possible damage scenario progression that would produce the observed variations in the ‘deltas’ with time. Since the precise damage to the Orbiter and its progression with time were not known during the accident investigation, several plausible scenarios that could lead to the observed deviations in aerodynamic coefficients were considered for the present computational study including:

- (1) Single or multiple missing RCC panel(s),
- (2) A gap behind an RCC panel that would allow hot gases to escape from wing lower surface to the upper surface,
- (3) Open landing gear well (due to missing landing gear door),
- (4) Dimpled wing lower surface, and
- (5) Distorted wing leading edge.

The FELISA software was used for the aerodynamic computations, and the aerodynamic coefficients and the corresponding ‘deltas’ were computed for the configurations listed above. One set of asymmetric flow computations was done to study the effect of sideslip angle on the ‘deltas’.

The FELISA Software

The FELISA unstructured grid software is a powerful tool that can be used to build grids for complex geometries and compute flow solutions within a few days. This software has been used extensively in the past for aerodynamic computations of flow past hypersonic and planetary entry vehicles.^{2,3} It has also been used successfully to compute high angle of attack (α greater than 40 degrees) aerodynamic coefficients of the Space Shuttle Orbiter.⁴ The software consists of a set of computer codes for unstructured grid generation, and simulation of three-dimensional steady, inviscid flows using unstructured tetrahedral grids, and post-processing of flow solutions. Surface triangulation and discretization of the computational domain using tetrahedral elements are done by using two separate codes. The surface and volume grids are isotropic with little or no stretching. Two flow solvers are available—one applicable for transonic flows, and the other for hypersonic flows. The hypersonic flow solver has options for perfect gas (constant γ), equilibrium air, CF_4 , CO_2 , and equilibrium gases representing Mars, Neptune, and Titan atmospheres. This solver also has the capability of solving chemical non-equilibrium flow and real gas (chemical and thermal non-equilibrium) flow. The hypersonic flow solver (with perfect gas air and CF_4 gas options) was used for the present computations. The FELISA flow solvers have been parallelized to run on multiprocessor machines. More information on FELISA software may be found in Peiro et al.⁵ A description of the hypersonic flow solver may be found in Bibb et al.⁶

Geometry

Since the Space Shuttle Orbiter has a plane of symmetry, computations were done on one half of the Orbiter. The ‘damaged’ Orbiter configurations, however, are all asymmetric. An examination of flow fields

of the baseline and damaged configurations suggested that the flow on the damaged side did not noticeably affect the flow on the undamaged side. The reason for this is that the damaged areas are small, and are located at a distance from the centerline. Therefore, it was decided to do the computations on only one half of the Orbiter. This not only reduced the required computer resources but also reduced the clock time by a factor of nearly 2. The present computations were done for the the following configurations:

1. *Baseline*: A sketch of the Orbiter baseline geometry is shown in Figure 1. In order to avoid computing the separated flow behind the fuselage, the OMS pod, the bodyflap, and the fin, pseudo surfaces were built to extend these surfaces all the way to the exit plane. This causes the flow leaving fuselage and other surfaces not to separate, but flow smoothly over the fake surfaces to the exit plane. In hypersonic flows, this does not affect the upstream flow and computed 'deltas'.

2. *Missing RCC Panel(s)*: Figure 2 shows the 'Panel 6 Out', 'Panels 6 & 7 Out', 'Panels 5, 6, & 7 Out', and 'Panel 9 Out' configurations. At the time when this work was started, the actual size of the RCC panels and their locations on the wing leading edge were not known. Approximate location and size of panel 6 were extracted from an old document, and were used for the first set of computations. This is the reason for the panel 6 being much smaller than it should be in Figure 2a. Precise location and size of all the panels were later obtained, and were used for all subsequent computations.

3. *Slots*: The effect of flow going through a slot behind panel 9 was studied. A sketch of the slot is shown in Figure 3. The length of the slot is 27.9 in. Slots of two different widths (0.53 in and 0.99 in) were studied.

4. *Open Landing Gear Well*: The next damaged configuration considered was the open landing gear well shown in Figure 4. The well was simplified to be a rectangular hole 151 in long and 62 in wide. Three cases were run with 6 in, 15 in, and 30 in for the depths of the landing gear well.

5. *Dimple*: The next damaged configuration studied was the 'dimple' (or a depression) on the underside of the wing near the RCC panel 9. The shape of the dimple was rectangular with the ends rounded as shown in Figure 5. Four dimple configurations were studied; all the dimples were 23 in wide. The first one of these is called the 'Long Dimple', and is 149.8 in long (Fig. 5a); the second is called the 'Short Dimple' and is 97.8 in long (Fig. 5b). Both of these were approximately 6 in deep. The third, called the 'Short Shallow Dimple', is 97.8 in long and only 3 in deep (Fig. 5c) The fourth configuration is the 'Long Dimple' with the Panel 9 Out (Fig. 5d).

6. *Damaged Wing Leading Edge*: In this case a part of the wing leading edge was assumed to be damaged as shown in Figure 6. The damage amounted to a change in the local angle of attack of the wing in the area shown. The wing leading edge was assumed to remain smooth.

7. *Full Vehicle*: A set of computations were done for the full vehicle to compute the effect of asymmetric flow (non-zero β). The only damaged scenario studied was the 'Panel 9 Out' case.

The right-handed axis system used here has the origin at the nose of the vehicle (see Figure 1). The x-axis and the z-axis are in the symmetry plane; the z-axis is along the body axis and points upstream, and the x-axis points up. The y-axis is perpendicular to the symmetry plane and points to the starboard side of the Orbiter. This axis system is used for all the configurations. The reference quantities used for non-dimensionalizing the aerodynamic loads are as follows:

Reference area, (S_{ref})	193,680 sq.in.
Reference length for CM_Y , (c_{ref})	474.72 in
Reference length for CM_X and CM_Z , (b_{ref})	936.684 in
Moment reference point	(38.5 in, 0, -841.7 in)
(that is 38.5 in above the centerline, on the symmetry plane, and 841.7 in behind the nose.)	

Grids Used in the Present Study

The starting point for building grids was a Space Shuttle Orbiter IGES file. The RCC panels and the damaged regions were defined by simple curves, and were also available in the IGES format. These IGES files

were processed using the software GridTool,⁷ and a set of FELISA data files was generated. These included: (1) the FELISA data file that contains all the information on the surface definition and the computational domain in a format suitable for the FELISA grid generator, (2) the FELISA background file that specifies the grid spacing, and (3) the FELISA boundary conditions file. The computational domain (see Figure 7) was chosen to be sufficiently large so that the inflow boundaries did not affect the flow on the body.

It was known at the outset that the ‘deltas’, which are the differences in the aerodynamic coefficients for the damaged vehicle and the corresponding coefficients for the undamaged or baseline vehicle were small. In order to capture these small quantities, large grids would be needed. Further, the grid spacing for the baseline and the damaged vehicles needed to be the same except in the region of the damage, so that two grids would be essentially the same except around the damaged region. This would insure that the resulting ‘deltas’ would be essentially due to the vehicle damage only.

The grid spacing was chosen to obtain dense gridding in regions of high gradients and sparse gridding in other places. In the freestream and in regions of very small gradients the grid spacing was 40 *in*, and in other places around the body it was much smaller (1 to 5 *in*). Around the fuselage nose the spacing was 0.2 *in*. This provided adequate grid resolution to capture the bow shock in front of the body. Around the wing leading edge the grid spacing varied from 1 to 2 *in*. For the ‘Slot’ configuration meshes the minimum grid spacing within and around the slot was 0.15 *in*.

Starting with the FELISA data files, unstructured surface triangulation and tetrahedral grids were generated using the surface and volume grid generators, respectively on an SGI Onyx. A new grid was built for each configuration. The grids for the full configuration were especially very large, consisting of over 34 million tetrahedral elements. The properties of all these grids are shown in Table 1.

The grid *Baseline* for the baseline configuration and *Baseline-6* for the panel 6 out configuration (See Table 1) have the same grid spacings, except around the panel 6. These grids were used for computations with perfect gas air. The grid *Base_cf4* for baseline and the grids for all panel out, slot, and open landing gear well cases have the same mesh spacing in the computational domain except near the damaged areas. For the computations with the ‘Dimple’ cases, a new grid *Base* was built for the baseline configuration. This grid and all the grids used for the dimple cases (namely *dimple*, *sdimple*, *ssdimple*, *p9dimple*) and *damage3* have the same mesh spacing except near the damaged areas.

Flow Solution

The flow solutions were computed on a Pentium based cluster. The grids were partitioned so that the solution could be run on 16 or 24 processors. The FELISA hypersonic flow solver with the perfect gas air ($\gamma=1.4$) and the CF_4 gas option were used for these computations. Each FELISA solution was started with solver’s low-order option, and after 2000 iterations, with solver’s higher-order option was turned on, and the solution was run to convergence. After every 100 iterations, the surface pressures were integrated, and the aerodynamic coefficients were computed. The flow solution was assumed to be converged when these integrated loads remained essentially constant. This required about 8,000 iterations and 200 hours of CPU time.

The flow conditions used for computations with the CF_4 gas corresponded to test conditions in the Langley CF4 tunnel, and are as follows:

Velocity, (V_∞)	2994 <i>ft/s</i> (=912.6 <i>m/s</i>)
Density, (ρ_∞)	2.926E-05 <i>slugs/ft³</i> (=1.509E-02 <i>kg/m³</i>)
Temperature, (T_∞)	387.4°R (=215.2 <i>K</i>)

All the computations were done for an angle of attack of 40 degrees. For the full model, computations were done for sideslip angles of -1, 0, and +1 degrees.

Aerodynamic loads obtained by integrating the surface pressures were non-dimensionalized in the conventional manner, and the aerodynamic coefficients, namely C_X , C_Y , C_Z , CM_X , CM_Y , and CM_Z were

obtained. The ‘deltas’ were computed by taking the differences between the coefficients for the damaged configurations and the corresponding coefficients for the baseline configuration. Thus, for C_X , we have

$$\delta C_X = (C_X)_{\text{damaged}} - (C_X)_{\text{baseline}}$$

and similar expressions for C_Y , C_Z , CM_X , CM_Y , and CM_Z .

Results and Discussion

The damaged configurations considered in the present study are such that they lead to locally large changes in pressure distribution on the wing leading edge. Therefore, the resulting ‘deltas’ (which are the difference between the aerodynamic coefficients for the damaged vehicle and the undamaged or baseline vehicle) are primarily due to pressure, and although the present computations are inviscid, the computed deltas are expected to be accurate. Further, it should be noted that these ‘deltas’ are very small. For example, for the Panel out cases the δCM_Z and the δCM_X are of the order of 0.001. These numbers are comparable to the accuracy associated with the CM_Z and the CM_X . However, as noted earlier, since the grids were designed specifically to capture the ‘deltas’, they are expected to be quite accurate. No attempt was made to check whether the results were grid converged.

Out of the six ‘deltas’, the δCM_X and δCM_Z were considered to be of primary importance. Hence, these two ‘deltas’ are examined in the following paragraphs.

The Half model Results:

Aerodynamic coefficients from the present computations for the baseline, and the damaged configurations on the half model are summarized in Tables 2 and 3, and the ‘deltas’ are summarized in Tables 4. The δCM_X and δCM_Z for all the damaged configurations are shown in Figures 8 and 9. It may be noted that the δCM_X for all the configurations are positive. Considering only the panel out cases (Figure 8), Panel 6 Out yields the least (0.09E-3) and Panel 9 Out gives the largest (1.42E-3) values for δCM_X . The δCM_Z values for all panel out cases are all negative, and Panel 5, 6, & 7 Out case yields largest values (-8.0E-4). As more number of panels are removed from the wing, the δCM_Z increases. This is possibly due to the fact that as more area is removed from the wing there is a corresponding reduction in the normal force, that leads to the δCM_Z . The δCM_X appears to depend on the spanwise location of the panels taken out. Forward facing area at the wing leading edge (due to the missing panels) experiences a high pressure leading to a moment about the x-axis. Moving this to outboard stations leads to δCM_X .

Contribution from the Slot and the Wider Slot to δCM_X and δCM_Z are small.

The ‘deltas’ for the three Landing Gear Well cases show an interesting trend. The δCM_X as well as the δCM_Z are positive for all the L.G. Well cases. The 15 in deep L.G. Well shows the largest values for both δCM_X (1.73E-3) and δCM_Z (0.72E-3). For the 6 in and 15 in deep L.G. Wells the corresponding δ are smaller.

For the four dimple cases, as well as the damaged wing leading edge cases, δCM_X as well as the δCM_Z are positive. In all these cases the wing underside was disturbed, causing the wing (underside) pressures to rise and produce a positive δCM_X . It is interesting to note that the ‘deltas’ for dimple & panel 9 removed configuration can be obtained with a simple addition of the ‘deltas’ for the dimple alone and the ‘deltas’ for panel 9 removed.

The ‘Full’ model Results:

Computations were done for the full configuration to compute the effect of sideslip on the ‘deltas’. First, computations were done for the baseline configuration for $\beta=-1, 0$, and $+1 \text{ deg.}$ and $\alpha=40 \text{ deg.}$ with the CF_4 tunnel conditions. Next, these computations were repeated for the damaged configuration with the RCC panel 9 removed from the port wing.

The upper and lower surface C_p distributions for $\beta=0 \text{ deg.}$ are shown in Figure 10a and 10b. It may be noted that while the absence of panel 9 changes the pressure distribution on the upper surface, whereas the

lower surface pressure distribution remains unaffected. The C_p distributions on the body on the damaged and undamaged sides are shown in Figure 11a and 11b. The flow going through the gap (due to missing panel 9) and directed towards the fuselage may be seen in Figure 10a. Impingement of such a flow on the fuselage side is the likely cause of the hot-spots recorded in the Orbiter flight data.

The aerodynamic coefficients for these configurations are listed in Table 5, and are shown plotted in Figures 12 and 13. The ‘deltas’ are listed in Table 6. Over the β range of -1 to +1 degrees, all the aerodynamic coefficients vary linear with β , and the ‘deltas’ are nearly constant. These ‘deltas’ (for panel 9 configuration) computed on the full model are comparable to the corresponding values obtained using the half model.

Acknowledgments

The work described herein was performed at Lockheed Martin Engineering & Sciences Company in Hampton, Virginia, and was supported by Aerothermodynamics Branch, NASA Langley Research Center under the contract NAS1-00135. The technical monitor was Dr. N. Ronald Merski. The author wishes to thank Karen L. Bibb for many helpful discussions during the course of this work.

References

- ¹“Columbia Accident Investigation Board Report,” Volume 1, August 2003, p. 9.
- ²Prabhu, R.K.: “Inviscid Flow Computations of the Orbital Sciences X-34 Over a Mach Number Range of 1.25 to 6.0” NASA/CR-2001-210849, April 2001.
- ³Prabhu, R.K.: “Inviscid Flow Computations of Two ’07 Mars Lander Aeroshell Configurations Over a Mach Number Range of 2 to 24,” NASA/CR-2001-210852, April 2001.
- ⁴Prabhu, R.K.: “Inviscid Flow Computations of the Space Shuttle Orbiter for Mach 10 and 15 and Angle of Attack 40 to 60 Degrees,” NASA/CR-2001-211267, December 2001.
- ⁵Peiro, J., Peraire, J., and Morgan, K.: “FELISA System Reference Manual and User’s Guide,” Technical Report, University College, Swansea, Wales, 1993, (Also NASA CP 3291, May 1995.)
- ⁶Bibb, K.L., Peraire, J., and Riley, C.J.: “Hypersonic Flow Computation on Unstructured Meshes,” AIAA Paper 97-0625, January 1997.
- ⁷Samereh, J.: “GridTool: A Surface Modeling and Grid Generation Tool,” NASA CP 3291, May 1995.

Configuration	Grid Name	No. of Points	No. of Triangles	No. of Tets	No. of Nodes
Baseline	<i>Baseline</i>	227,478	113,741	14,397,123	2,436,675
Panel 6 Out	<i>Baseline-6</i>	230,956	115,480	14,502,499	2,455,381
Baseline	<i>Base_cf4</i>	358,092	179,048	17 million	2,999,211
Panel 6 Out	<i>Base_cf4.6</i>	347,526	173,765	17,261,782	2,941,844
Panels 6 & 7 Out	<i>Base_cf4.67</i>	340,870	170,437	17,420,293	2,965,840
Panels 5, 6, & 7 Out	<i>Base_cf4.567</i>	342,444	171,224	17,510,427	2,981,318
Panel 9 Out	<i>Base_cf4.9</i>	340,136	170,070	17,467,887	2,973,650
Slot	<i>slot_cf9</i>	425,958	212,979	14,044,231	2,429,516
Wider Slot	<i>Wslot_cf9</i>	471,274	235,637	22,037,778	3,760,853
L.G. Well, 6" Deep	<i>door6</i>	342,260	171,132	17,093,737	2,913,683
L.G. Well, 15" Deep	<i>door15</i>	347,516	173,760	16,969,322	2,894,275
L.G. Well, 30" Deep	<i>door30</i>	354,408	177,206	17,631,557	3,005,540
Baseline	<i>Base</i>	237,984	118,994	14,638,278	2,479,392
Dimple	<i>dimple</i>	289,470	144,737	15,705,294	2,669,783
Short Dimple	<i>sdimple</i>	270,514	135,259	15,288,618	2,595,904
Short Shallow Dimple	<i>ssdimple</i>	264,954	132,479	15,218,857	2,582,882
Dimple & Panel 9 Out	<i>p9dimple</i>	270,224	135,114	13,035,429	2,223,760
Damaged LE	<i>damage3</i>	234,256	117,130	14,531,093	2,460,779
Baseline	<i>full_cf4</i>	605,450	302,727	34,605,278	5,872,566
Panel 9 Out	<i>full_cf9</i>	607,280	303,642	34,757,554	5,898,267

Table 1 Properties of grids used in the present computations.

Configuration	C_X	C_Y	C_Z	CM_X	CM_Y	CM_Z
Baseline	1.2635	1.5298E-01	-4.7708E-02	-2.9344E-02	-5.4721E-02	1.8623E-01
Panel 6 Out	1.2623	1.5301E-01	-4.8661E-02	-2.9422E-02	-5.5202E-02	1.8579E-01

Table 2 Aerodynamic coefficients for baseline and ‘Panel 6 Out’ configurations, Perfect Gas Air, M=6, $\alpha=40$ deg.

Configuration	C_X	C_Y	C_Z	CM_X	CM_Y	CM_Z
Baseline	1.2353	1.5413E-01	-5.1355E-02	-3.0274E-02	-2.7207E-02	1.7772E-01
Panel 6 Out	1.2345	1.5427E-01	-5.3352E-02	-3.0102E-02	-2.8058E-02	1.7753E-01
Panels 6 & 7 Out	1.2286	1.5341E-01	-6.0480E-02	-2.9077E-02	-2.9308E-02	1.7633E-01
Panels 5, 6, & 7 Out	1.2263	1.5363E-01	-6.3677E-02	-2.8128E-02	-3.0189E-02	1.7612E-01
Panel 9 Out	1.2288	1.5475E-01	-5.9921E-02	-2.7435E-02	-2.7769E-02	1.7709E-01
Slot	1.2371	1.5452E-01	-5.1685E-02	-2.9734E-02	-2.9760E-02	1.7734E-01
Wider Slot	1.2372	1.5465E-01	-5.1795E-02	-2.9655E-02	-2.9619E-02	1.7735E-01
L.G. Well, 6” Deep	1.2468	1.5237E-01	-6.4568E-02	-2.7925E-02	-3.4559E-02	1.7890E-01
L.G. Well, 15” Deep	1.2488	1.4863E-01	-7.4180E-02	-2.6806E-02	-3.4120E-02	1.7915E-01
L.G. Well, 30” Deep	1.2400	1.5371E-01	-5.8086E-02	-2.8897E-02	-2.9841E-02	1.7778E-01
Baseline	1.2372	1.5425E-01	-5.1508E-02	-2.9758E-02	-2.9786E-02	1.7739E-01
Dimple	1.2424	1.5255E-01	-5.5533E-02	-2.8742E-02	-3.2511E-02	1.7875E-01
Short Dimple	1.2398	1.5251E-01	-5.5451E-02	-2.8850E-02	-3.0767E-02	1.7807E-01
Short Shallow Dimple	1.2388	1.5342E-01	-5.3689E-02	-2.9295E-02	-3.0309E-02	1.7783E-01
Dimple & Panel 9 Out	1.2364	1.5434E-01	-6.3901E-02	-2.5754E-02	-3.3010E-02	1.7824E-01
Damaged Wing	1.2385	1.5741E-01	-5.4966E-02	-2.8747E-02	-3.0378E-02	1.7739E-01

Table 3 Aerodynamic coefficients for Baseline and several damaged configurations, CF_4 gas, M=5.85, $\alpha=40$ deg.

Model	Gas	δC_X	δC_Y	δC_Z	δCM_X	δCM_Y	δCM_Z
Panel 6 Out	Air	-1.20E-03	0.03E-03	-0.95E-03	0.08E-03	-0.48E-03	0.44E-03
Panel 6 Out	CF_4	-0.40E-03	0.07E-03	-1.00E-03	0.09E-03	-0.43E-03	-0.10E-03
Panels 6 & 7 Out	CF_4	-3.35E-03	-0.36E-03	-4.56E-03	0.60E-03	-1.05E-03	-0.70E-03
Panels 5, 6, & 7 Out	CF_4	-4.50E-03	-0.25E-03	-6.16E-03	1.07E-03	-1.49E-03	-0.80E-03
Panel 9 Out	CF_4	-3.25E-03	0.31E-03	-4.28E-03	1.42E-03	-0.28E-04	-0.32E-03
Slot	CF_4	0.90E-03	0.20E-03	-0.17E-03	0.27E-03	-1.28E-03	-0.19E-03
Wider Slot	CF_4	0.95E-03	0.26E-03	-0.22E-03	0.31E-03	-1.21E-03	-0.19E-03
L.G. Well, 6" Deep	CF_4	5.75E-03	-0.88E-03	-6.61E-03	1.17E-03	-3.68E-03	0.59E-03
L.G. Well, 15" Deep	CF_4	6.75E-03	-2.75E-03	-11.4E-03	1.73E-03	-3.46E-03	0.71E-03
L.G. Well, 30" Deep	CF_4	2.35E-03	-0.21E-03	-3.37E-03	0.69E-03	-1.32E-03	0.03E-03
Dimple	CF_4	2.60E-03	-0.85E-03	-2.01E-03	0.51E-03	-1.36E-03	0.68E-03
Short Dimple	CF_4	1.30E-03	-0.87E-03	-1.97E-03	0.45E-03	-0.49E-03	0.34E-03
Short Shallow Dimple	CF_4	0.80E-03	-0.42E-03	-1.09E-03	0.23E-03	-0.26E-03	0.22E-03
Dimple & Panel 9 Out	CF_4	-0.40E-03	0.05E-03	-6.20E-03	2.00E-03	-1.61E-03	0.43E-03
Damaged Wing	CF_4	0.65E-03	1.58E-03	-1.73E-03	0.51E-03	-0.30E-03	0.00E-00

Table 4 The ‘deltas’ for the damaged configurations at $\alpha=40$ deg.

Config.	β <i>deg</i>	C_X	C_Y	C_Z	CM_X	CM_Y	CM_Z
Baseline	+1	1.2351	5.4679E-03	-5.1542E-02	-1.2911E-03	-2.6805E-02	1.4204E-03
Baseline	0	1.2351	-2.0009E-05	-5.1534E-02	3.2192E-06	-2.6757E-02	1.2426E-05
Baseline	-1	1.2352	-5.4895E-03	-5.1539E-02	1.3039E-03	-2.6781E-02	-1.4011E-03
Panel 9 Out	+1	1.2317	5.9294E-03	-5.5943E-02	2.2551E-04	-2.7191E-02	1.1316E-03
Panel 9 Out	0	1.2317	5.4120E-04	-5.5853E-02	1.5334E-03	-2.7122E-02	-2.4101E-04
Panel 9 Out	-1	1.2318	-4.8427E-03	-5.5777E-02	2.8523E-03	-2.7124E-02	-1.6106E-03

Table 5 Aerodynamic coefficients for the full model, CF_4 gas, $M=5.85$, $\alpha=40$ deg.

Config.	β <i>deg</i>	δC_X	δC_Y	δC_Z	δCM_X	δCM_Y	δCM_Z
Full	+1	-3.40E-03	0.46E-03	-4.40E-03	1.52E-03	-0.39E-03	-0.29E-03
Full	0	-3.40E-03	0.56E-03	-4.32E-03	1.53E-03	-0.37E-03	-0.25E-03
Full	-1	-3.40E-03	0.65E-03	-4.24E-03	1.55E-03	-0.34E-03	-0.21E-03

Table 6 The ‘deltas’ for the wing Panel 9 Out configuration, CF_4 gas, $M=5.85$, $\alpha=40$ deg.

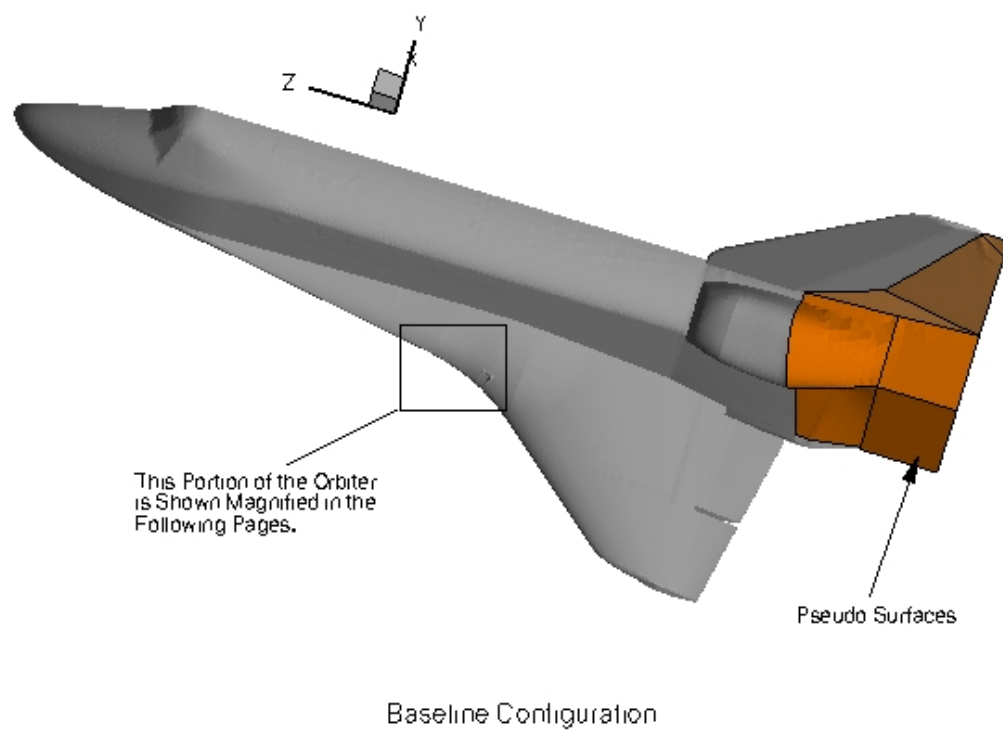


Fig. 1 The 'Baseline' configuration.

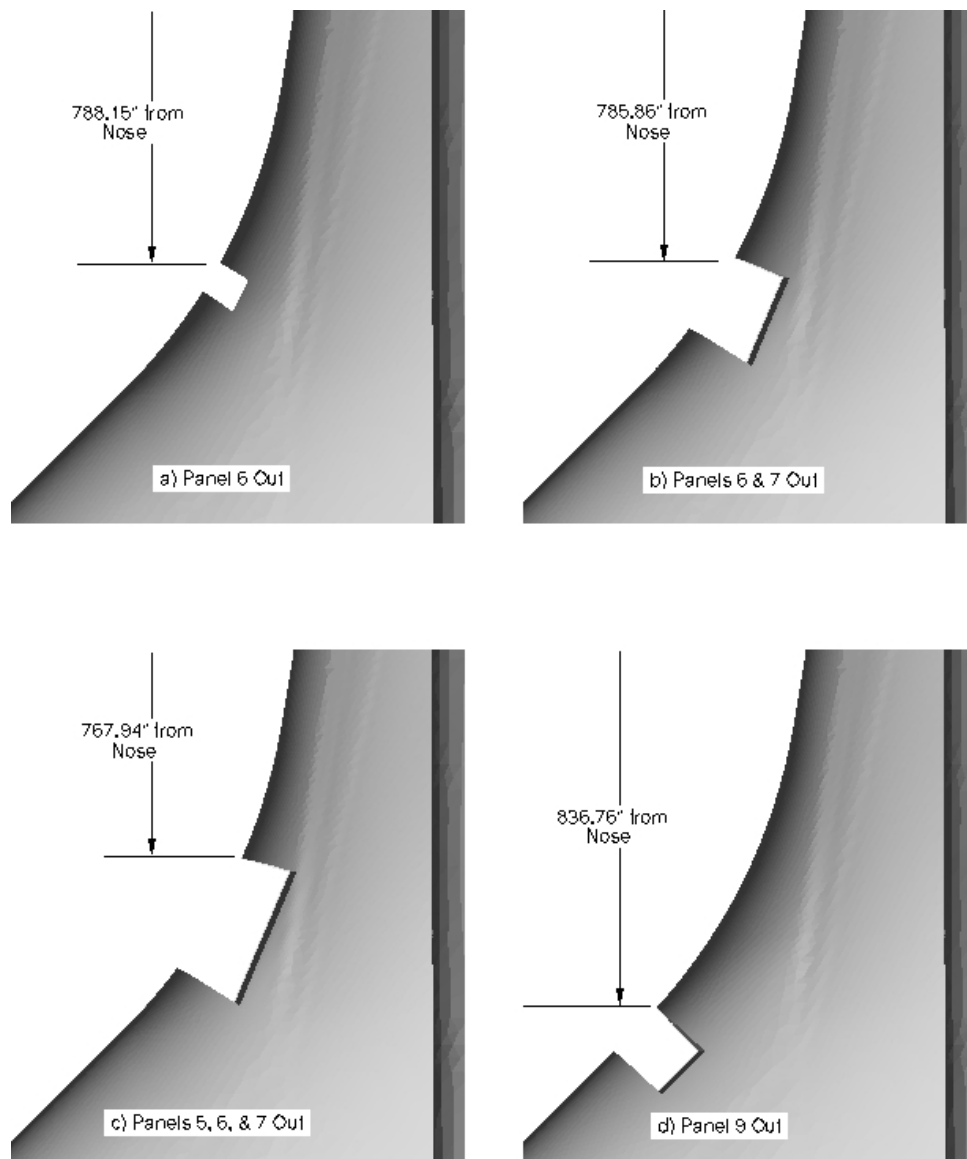


Fig. 2 The RCC panels.

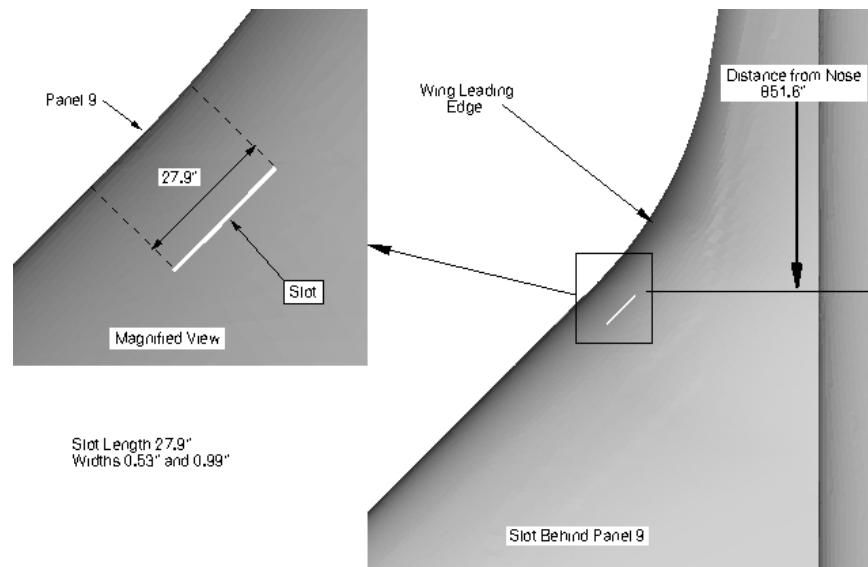


Fig. 3 The 'Slot' configuration.

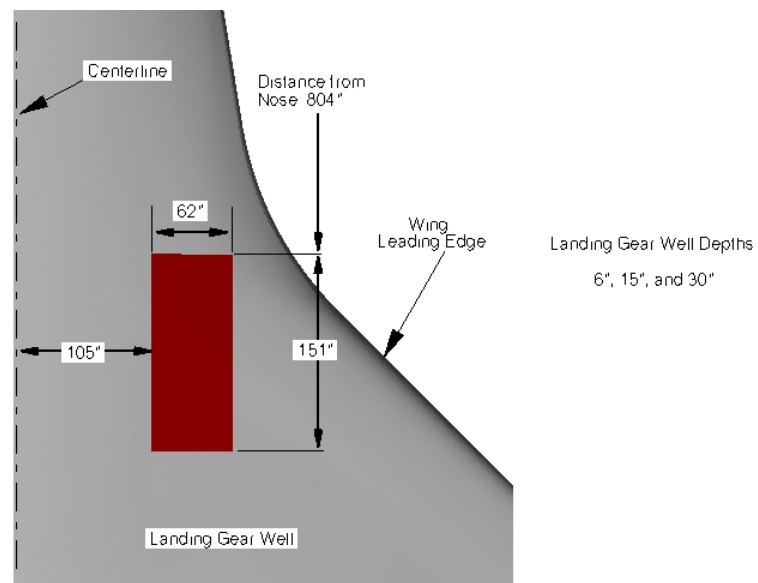


Fig. 4 The landing gear well.

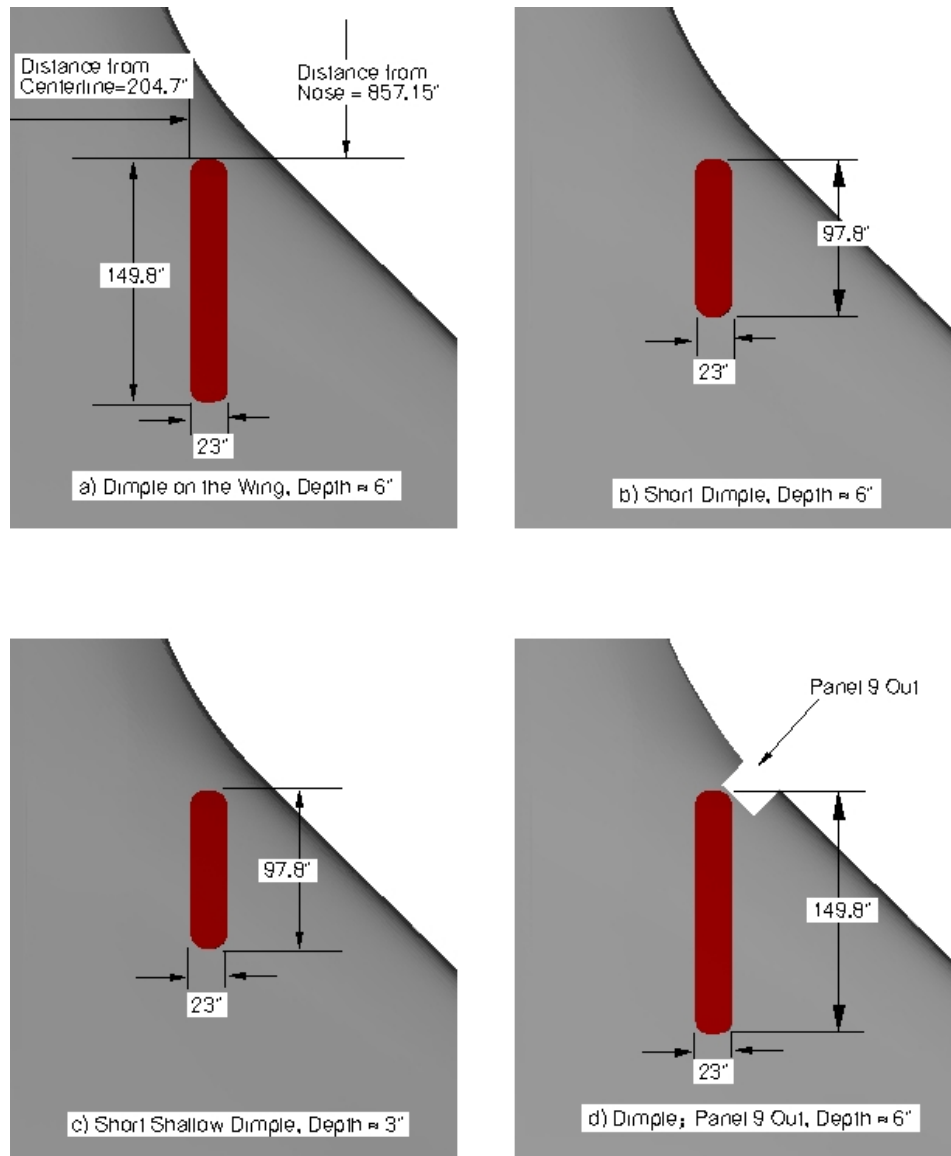


Fig. 5 The 'Dimple' configurations.

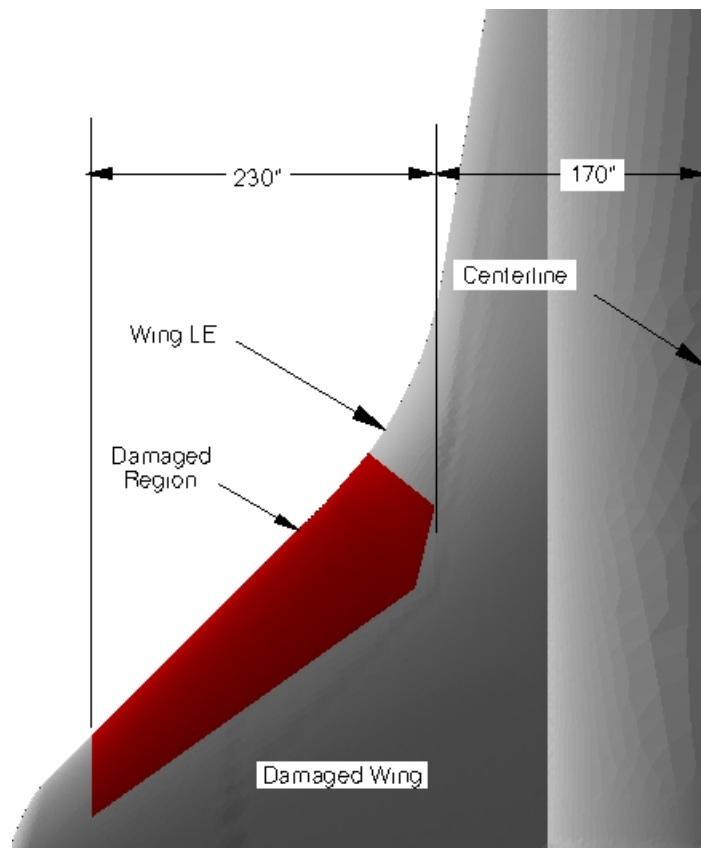


Fig. 6 The 'Damage' configuration.

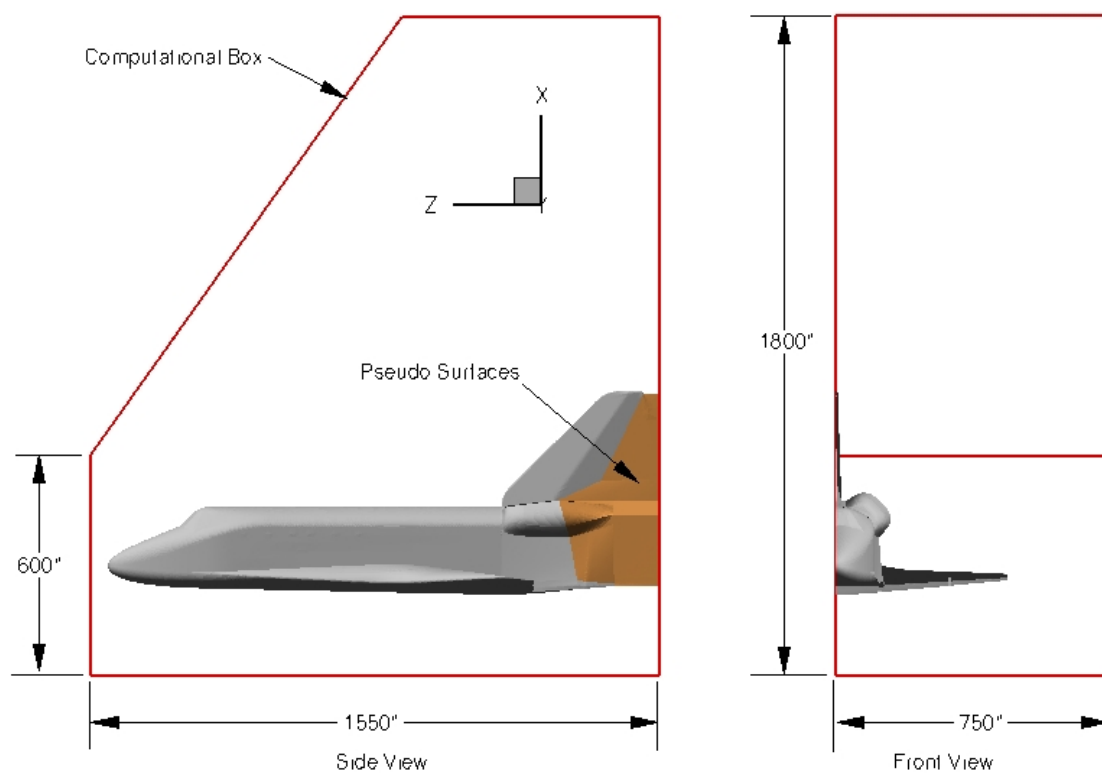


Fig. 7 The computational domain.

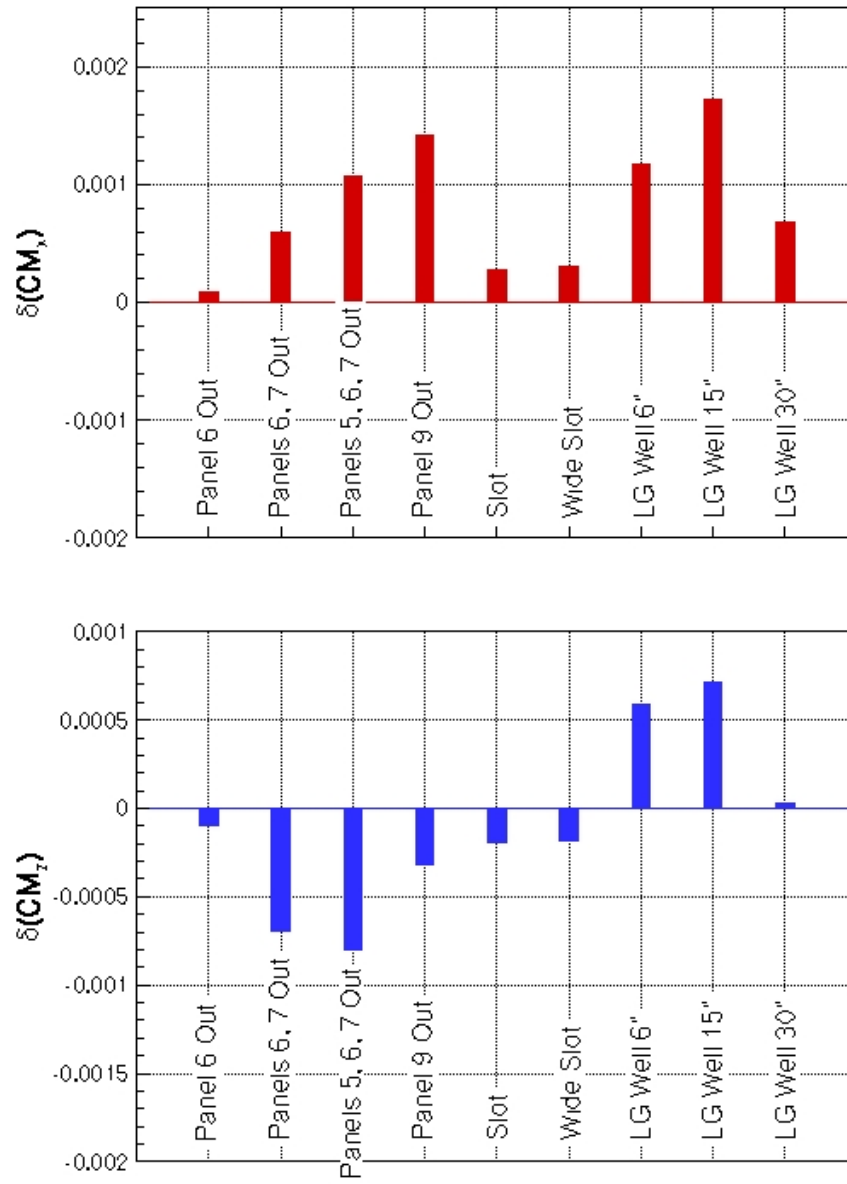


Fig. 8 δCM_X and δCM_Z for panel out, slot, and landing gear well Configurations.

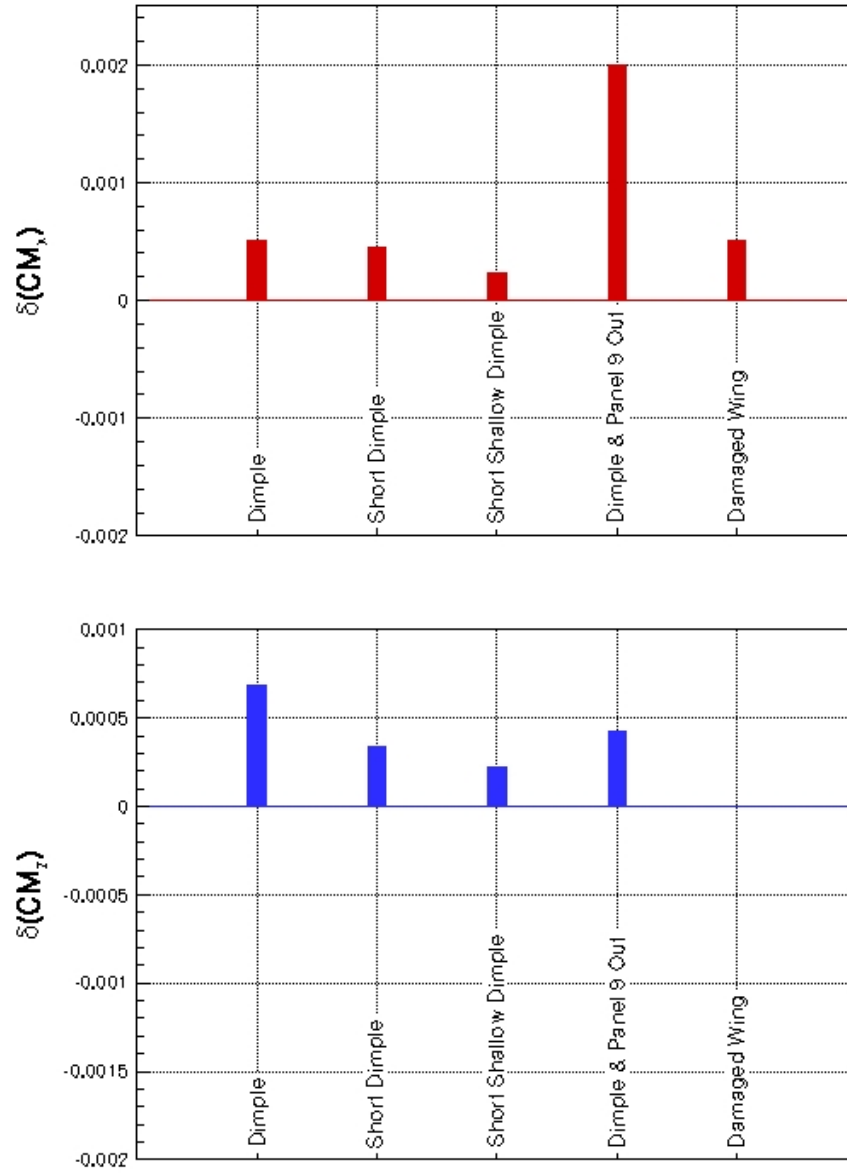


Fig. 9 δCM_X and δCM_Z for Dimple and Damaged wing configurations.

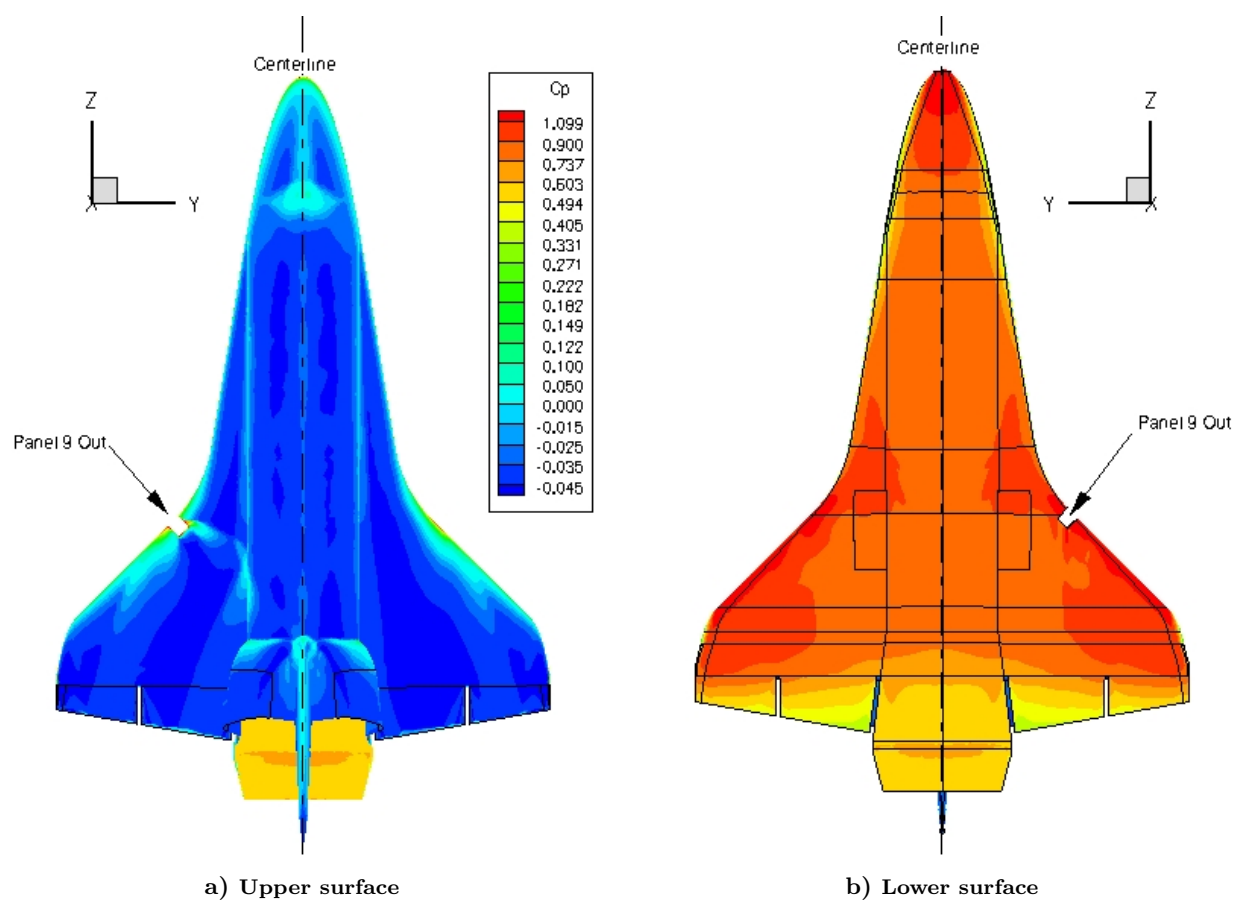


Fig. 10 Wing surface C_p distributions for the full model, CF_4 gas, $M=5.85$, $\alpha=40$ deg., $\beta=0$ deg.

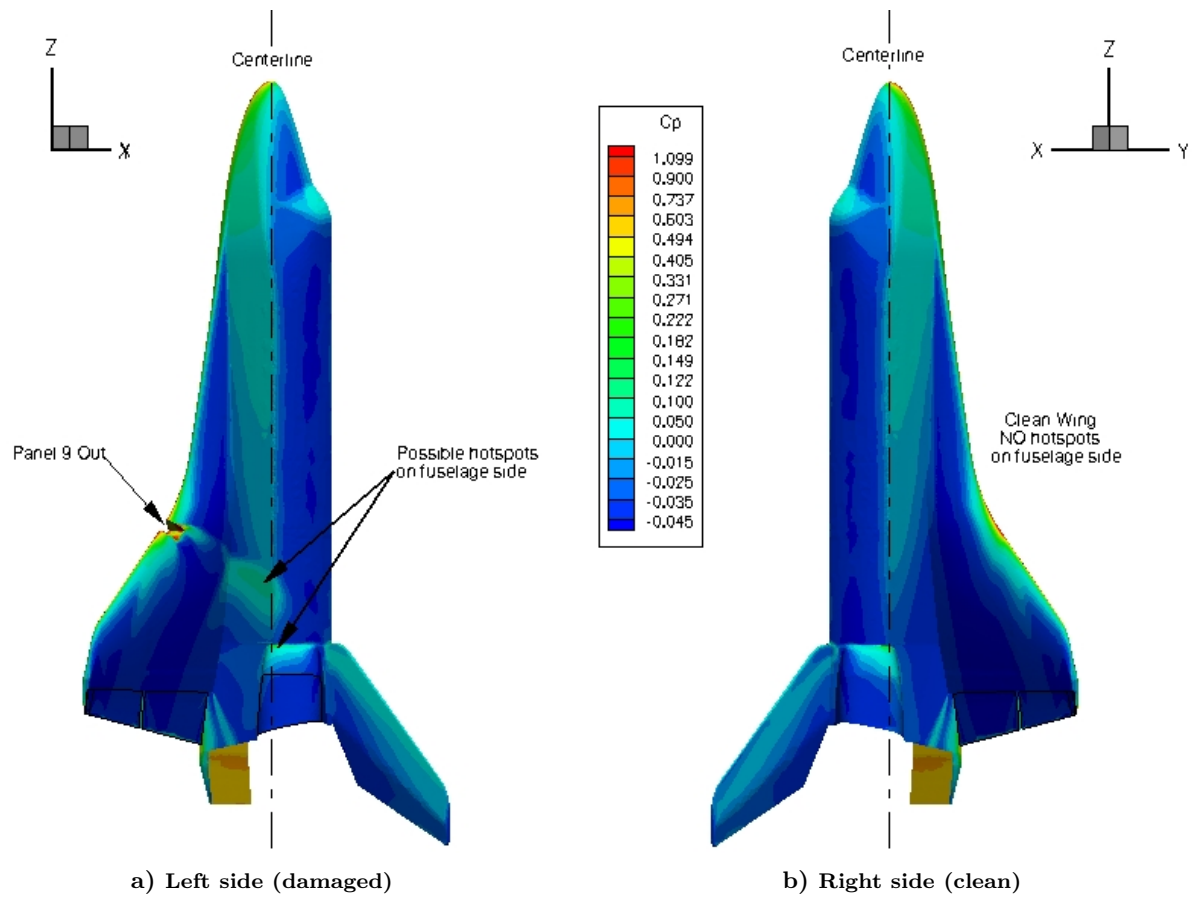


Fig. 11 Body surface C_p distributions for the full model, CF_4 gas, $M=5.85$, $\alpha=40^\circ$, $\beta=0^\circ$.

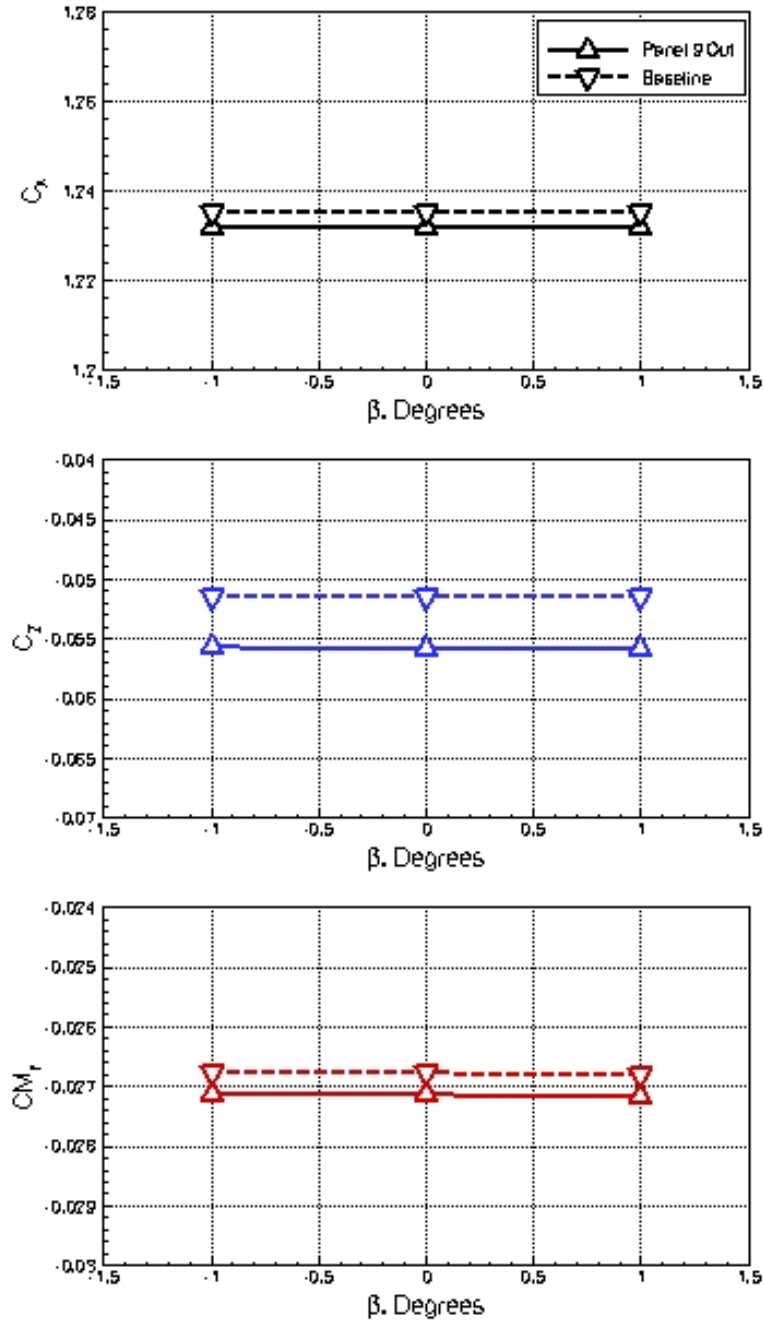


Fig. 12 Variation of C_x , C_z , and CM_Y with β for the Baseline and Panel 9 Out configurations, CF_4 gas, $M=5.85$, $\alpha=40$ deg.

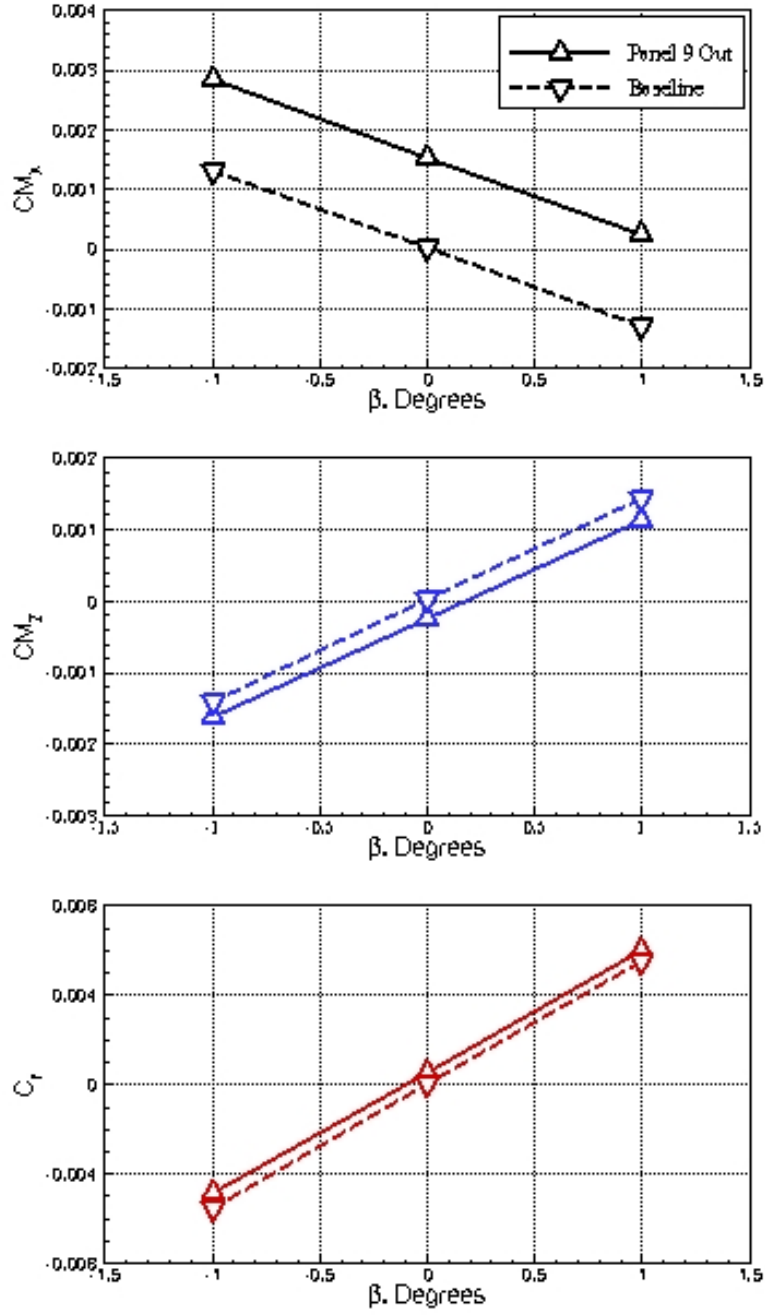


Fig. 13 Variation of CM_x , CM_z , and C_y with β for the baseline and Panel 9 Out configurations, CF_4 gas, $M=5.85$, $\alpha=40$ deg.

REPORT DOCUMENTATION PAGE					Form Approved OMB No. 0704-0188	
<p>The public reporting burden for this collection of information is estimated to average 1 hour per response, including the time for reviewing instructions, searching existing data sources, gathering and maintaining the data needed, and completing and reviewing the collection of information. Send comments regarding this burden estimate or any other aspect of this collection of information, including suggestions for reducing this burden, to Department of Defense, Washington Headquarters Services, Directorate for Information Operations and Reports (0704-0188), 1215 Jefferson Davis Highway, Suite 1204, Arlington, VA 22202-4302. Respondents should be aware that notwithstanding any other provision of law, no person shall be subject to any penalty for failing to comply with a collection of information if it does not display a currently valid OMB control number.</p> <p>PLEASE DO NOT RETURN YOUR FORM TO THE ABOVE ADDRESS.</p>						
1. REPORT DATE (DD-MM-YYYY)		2. REPORT TYPE		3. DATES COVERED (From - To)		
01- 07 - 2004		Contractor Report				
4. TITLE AND SUBTITLE An Inviscid Computational Study of the Space Shuttle Orbiter and Several Damaged Configurations				5a. CONTRACT NUMBER		
				NAS1-00135		
				5b. GRANT NUMBER		
6. AUTHOR(S) Prabhu, Ramadas K.				5c. PROGRAM ELEMENT NUMBER		
				5d. PROJECT NUMBER		
				5e. TASK NUMBER		
7. PERFORMING ORGANIZATION NAME(S) AND ADDRESS(ES) NASA Langley Research Center Swales Aerospace Hampton, VA 23681-2199 Hampton, VA 23666				5f. WORK UNIT NUMBER		
				SFCX22004D		
				8. PERFORMING ORGANIZATION REPORT NUMBER		
9. SPONSORING/MONITORING AGENCY NAME(S) AND ADDRESS(ES) National Aeronautics and Space Administration Washington, DC 20546-0001				10. SPONSOR/MONITOR'S ACRONYM(S)		
				NASA		
12. DISTRIBUTION/AVAILABILITY STATEMENT Unclassified - Unlimited Subject Category 02 Availability: NASA CASI (301) 621-0390 Distribution: Standard				11. SPONSOR/MONITOR'S REPORT NUMBER(S)		
				NASA/CR-2004-213241		
13. SUPPLEMENTARY NOTES Langley Technical Monitor: N. R. Merski, Jr. An electronic version can be found at http://techreports.larc.nasa.gov/ltrs/ or http://ntrs.nasa.gov						
14. ABSTRACT Inviscid aerodynamic characteristics of the Space Shuttle Orbiter were computed in support of the Columbia Accident Investigation. The unstructured grid software FELISA was used and computations were done using freestream conditions corresponding to those in the NASA Langley 20-Inch Mach 6 CF4 tunnel test section. The angle of attack was held constant at 40 degrees. The baseline (undamaged) configuration and a large number of damaged configurations of the Orbiter were studied. Most of the computations were done on a half-model. However, one set of computations was done using the full-model to study the effect of sideslip. The differences in the aerodynamic coefficients for the damaged and the baseline configurations were computed. Simultaneously with the computation reported here, tests were being done on a scale model of the Orbiter in the 20-Inch Mach 6 CF4 tunnel to measure the 'deltas'. The present computations complemented the CF4 tunnel test, and provided aerodynamic coefficients of the Orbiter as well as its components. Further, they also provided details of the flow field.						
15. SUBJECT TERMS Aerodynamic Loads; Hypersonics; Shuttle Accident Investigation; Space Shuttle Orbiter; Unstructured Grid CFD						
16. SECURITY CLASSIFICATION OF:			17. LIMITATION OF ABSTRACT	18. NUMBER OF PAGES	19a. NAME OF RESPONSIBLE PERSON	
a. REPORT	b. ABSTRACT	c. THIS PAGE			STI Help Desk (email: help@sti.nasa.gov)	
U	U	U	UU	27	19b. TELEPHONE NUMBER (Include area code) (301) 621-0390	